Two-Body Hadronic Weak Decays of Bottomed Hadrons

Ying Zhang(张颖)[1,2], Guangzhao He(何广朝)[1,2], Quanxing Ye(叶全兴)[1,2], Da-Cheng Yan(严大程)[3*], Jun Hua(华俊)[1,2*], and Qian Wang(王倩)[1,2,4*]

[1]*Key Laboratory of Atomic and Subatomic Structure and Quantum Control (MOE), Guangdong Basic Research Center of Excellence for Structure and Fundamental Interactions of Matter, Institute of Quantum Matter, South China Normal University, Guangzhou 510006, China*

[2]*Guangdong-Hong Kong Joint Laboratory of Quantum Matter, Guangdong Provincial Key Laboratory of Nuclear Science, Southern Nuclear Science Computing Center, South China Normal University, Guangzhou 510006, China*

[3]*School of Mathematics and Physics, Changzhou University, Changzhou 213164, China*

[4]*Southern Center for Nuclear-Science Theory (SCNT), Institute of Modern Physics, Chinese Academy of Sciences, Huizhou 516000, China*

(Received 25 October 2023; accepted manuscript online 29 December 2023)

The structure of light diquarks plays a crucial role in formation of exotic hadrons beyond the conventional quark model, especially with regard to the line shapes of bottomed hadron decays. We study the two-body hadronic weak decays of bottomed baryons and bottomed mesons to probe the light diquark structure and to pin down the quark–quark correlations in the diquark picture. It is found that the light diquark does not favor a compact structure. For instance, the isoscalar diquark $[ud]$ in Λ_b^0 can be easily split and rearranged to form $\Sigma_c^{(*)}\bar{D}^{(*)}$ via the color-suppressed transition. This provides a hint that the hidden charm pentaquark states produced in Λ_b^0 decays could be the $\Sigma_c^{(*)}\bar{D}^{(*)}$ hadronic molecular candidates. This quantitative study resolves the apparent conflicts between the production mechanism and the molecular nature of these P_c states observed in experiment.

DOI: 10.1088/0256-307X/41/2/021301

The strong interaction dynamics, namely quantum chromodynamics (QCD), does not eliminate the existence of more profound objects beyond hadrons in the conventional quark model picture, although the success of the conventional quark model indicates that a meson is made of a quark and anti-quark pair and a baryon is made of three quarks.[1,2] Since the observation of $X(3872)$ in 2003,[3] numerous exotic candidates that do not fit into the conventional quark model spectrum have been observed in experiment, such as $Z(3930)$,[4] $Y(4140)$,[5] $X(4500)$,[6] $P_c(4312)$, $P_c(4440)$, and $P_c(4457)$.[7] For reviews of exotic candidates in experiment, we recommend Refs. [8–17] Among these observations, the hidden charm pentaquarks, $P_c(4312)$, $P_c(4440)$, and $P_c(4457)$, observed by the LHCb collaboration,[7] are ideal hadronic molecular candidates for $\Sigma_c^{(*)}\bar{D}^{(*)}$, since their masses are close to the $\Sigma_c^{(*)}\bar{D}^{(*)}$ threshold and the $\Sigma_c^{(*)}\bar{D}^{(*)}$ interactions turn out to be attractive near the threshold.[18–52] However, whether these hidden charm pentaquarks behave as peaks or dips depends not only on the interaction force but also on the production amplitudes.[53] That is to say, it is not obvious that these P_c states in the molecular picture would favor their production in $\Lambda_b \to J/\psi p K$. Since Λ_b is an isoscalar, the production of $\Sigma_c^{(*)}\bar{D}^{(*)}$ in the Λ_b hadronic weak decays can only be through the light diquark violation process. This problem was first pointed out in Ref. [54]. It was also mentioned in Ref. [54] that, supposing that the $[ud]$ diquark within Λ_b is a compact object, the production of these P_c states will be extremely suppressed. In other words, the observation of these P_c states in the hadronic molecule scenario implies that the $[ud]$ diquark cannot be a compact object in space. Instead, the quantum correlation between the light quarks should be the key to resolving the contradictions when putting all the dynamics together.

In order to further clarify the role played by the light diquark configuration in the production of the hidden charm P_c states in the molecular picture, we investigate the two-body hadronic weak decays of the heavy flavor baryons and mesons, i.e., Λ_b, $\bar{B}_s^0$, Ξ_b^0, $\bar{B}^0$, Ξ_b^-, and B^-, by implementing the SU(3)-flavor symmetry. In fact, it has been pointed out that both Λ_c and Σ_c can be produced in Λ_b decays.[54] Taking the emergence of hidden charm pentaquarks as an example, the $\Lambda_b \to \Lambda_c^{(*)}\bar{D}^{(*)}K^-$ process can occur with the $[ud]$ diquark as a spectator, while the $\Lambda_b \to \Sigma_c^{(*)}\bar{D}^{(*)}K^-$ process violates the diquark model and can happen via the two processes illustrated in Figs. 1(b) and 1(c) of Ref. [54]. This mechanism has also been pointed out in Ref. [55]. However, due to the nonperturbative behavior of QCD, it is difficult to calculate the amplitude quantitatively. In this Letter, we investigate the validity of the diquark model for the two-body decay of bottomed mesons and baryons, which gives a hint of the significance of the $\Lambda_b \to \Sigma_c^{(*)}\bar{D}^{(*)}K^-$ process. In the following, we first present the framework, then provide the numerical results and related discussions. Finally, we give a brief summary.

Formalism. Because of the lack of experimental data on three-body decay for bottomed hadrons in the review of particle physics,[56] we resort to investigating their two-body decays. Since the spin singlet $[ud]$, $[us]$, $[sd]$ diquarks

*Corresponding authors. Email: yandac@126.com; junhua@m.scnu.edu.cn; qianwang@m.scnu.edu.cn

© 2024 Chinese Physical Society and IOP Publishing Ltd

conjugate to $\bar{s}$, $\bar{d}$, $\bar{u}$ quarks, respectively, according to the $SU(3)$ group theory, one can simultaneously study the decays of Λ_b^0, Ξ_b^0, Ξ_b^-, $\bar{B}_s^0$, $\bar{B}^0$, and B^-. Their lifetimes, total decay widths, and masses are collected in Text C in the Supplementary Material. In order to construct a simple but more general model, we only consider the contributions from the dominant tree-level diagrams, while those from the W-exchanged, annihilation, or penguin diagrams are usually expected to be small [57–59] and have been neglected in our calculations. For instance, the decays $\bar{B}_s^0 \to D^0\pi^0$, D^+D^-, etc., which can occur only through the annihilation diagrams, will not be analyzed in the current work. The two-body decay partial width reads

$$d\Gamma = \frac{(2\pi)^4}{2M}|\bar{\mathcal{M}}|^2 d\Phi_2(p_1; p_2, p_3), \tag{1}$$

with M being the mass of decaying particle, $\bar{\mathcal{M}}$ the spin-averaged decay amplitude, and $d\Phi_2$ the two-body phase space. Here, p_1, p_2, and p_3 are the momenta of the initial decay particle and the two final ones, respectively. As the polarization of the initial particle and final particles will be averaged and summed, the phase space integration is trivial and gives

$$\Gamma = \frac{1}{8\pi M^2}|\boldsymbol{p}||\bar{\mathcal{M}}|^2. \tag{2}$$

Here, $\boldsymbol{p}$ is the momentum of the two final states in the rest frame of the decaying particle. For decays whose partial decay widths are not measured experimentally, their momenta can be obtained by

$$|\boldsymbol{p}| = \frac{\sqrt{[M^2-(m_1+m_2)^2][M^2-(m_1-m_2)^2]}}{2M}, \tag{3}$$

with $m_{1,2}$ being the masses corresponding to the two final particles, respectively. The decay amplitude, $\bar{\mathcal{M}}$, will be parameterized as the diquark conserved and violation parts, for which we use the Λ_b and $\bar{B}_s^0$ decays as an example to illustrate the parameterization scheme. The decay mechanism is based on the leading-order contribution of the effective weak Hamiltonian, [60] i.e., the W-emitted diagram. The diquark conserved and violation diagrams are presented in Fig. 1. The diquark conserved amplitude shown in Fig. 1(a) reads

$$\bar{\mathcal{M}}^{\text{conserved}}(\Lambda_b^0 \to \Lambda_c^+\pi^-) = \frac{G_F}{\sqrt{2}}V_{cb}V_{ud}^*\mathcal{M}_a, \tag{4}$$

with Fermi coupling constant $G_F = 1.17\times10^{-5}\,\text{GeV}^{-2}$ [56] and the factor $\frac{1}{\sqrt{2}}$ from the standard effective weak Hamiltonian, [61] and $\mathcal{M}_a$ the amplitude parameter for the diagram keeping the light diquark structure. As shown in Fig. 1(a), the $[ud]$ diquark behaves as a spectator. V_{cb} and V_{ud}^* are the Cabibbo–Kobayashi–Maskawa (CKM) matrix elements. The diquark violation diagram is shown in Fig. 1(b), and the contribution of its decay to $\Lambda_c^+\pi^-$ and $\Sigma_c^+\pi^-$ can be obtained by Rach rearrangement, which has been successfully used for double charm baryon decays. [62,63] In Fig. 1(b), both the isospin and spin of the initial $[ud]$ light diquark in Λ_b are zero, which is denoted as $|ud_1\rangle_{(0,0)}$. The two subindexes in the parentheses are for the isospin and its third component. The $|d_2\bar{u}\rangle_{(1,-1)}$ diquark with isospin 1 and its third component -1 is created by the weak effective vertex, or more fundamentally by the W-emitted diagram. The subindexes 1 and 2 of the d quark mean that the d quark is from the initial bottom baryon and created from the weak vertex, respectively. By performing Rach rearrangement (for details see Text A in the Supplementary Material), one obtains

$$\begin{aligned}
&|ud_1\rangle_{(0,0)}|d_2\bar{u}\rangle_{(1,-1)}\\
&=\frac{1}{2}|ud_2\rangle_{(0,0)}|d_1\bar{u}\rangle_{(1,-1)} - \frac{1}{2}|ud_2\rangle_{(1,-1)}|d_1\bar{u}\rangle_{(0,0)}\\
&\quad+\frac{1}{\sqrt{2}}|ud_2\rangle_{(1,0)}|d_1\bar{u}\rangle_{(1,-1)}\\
&\Rightarrow \frac{1}{2}\Lambda_c^+\pi^- - \frac{1}{2}\Sigma_c^0\eta + \frac{1}{\sqrt{2}}\Sigma_c^+\pi^-.
\end{aligned} \tag{5}$$

Note that the isospins of the $[ud_2]$ diquark in the first and third terms are singlet and triplet, respectively, and will be hadronized into Λ_c^+ and Σ_c^+. Following Eq. (5), one can obtain the decay amplitudes

$$\bar{\mathcal{M}}^{\text{violation}}(\Lambda_b \to \Lambda_c^+\pi^-) = \frac{G_F}{\sqrt{2}}V_{cb}V_{ud}^*\frac{1}{2}\mathcal{M}_b, \tag{6}$$

$$\bar{\mathcal{M}}^{\text{violation}}(\Lambda_b \to \Sigma_c^0\eta) = -\frac{G_F}{\sqrt{2}}V_{cb}V_{ud}^*\frac{1}{2}\mathcal{M}_b, \tag{7}$$

$$\bar{\mathcal{M}}^{\text{violation}}(\Lambda_b \to \Sigma_c^+\pi^-) = \frac{G_F}{\sqrt{2}}V_{cb}V_{ud}^*\frac{1}{\sqrt{2}}\mathcal{M}_b, \tag{8}$$

from the light diquark violation diagram, with $\mathcal{M}_b$ being the amplitude parameter for the diagram breaking the light diquark structure. The total amplitude for a given process is the sum of the light diquark conserved and violation contributions, e.g.,

$$\begin{aligned}
\bar{\mathcal{M}}(\Lambda_b^0 \to \Lambda_c^+\pi^-) &= \bar{\mathcal{M}}^{\text{conserved}}(\Lambda_b \to \Lambda_c^+\pi^-)\\
&\quad+\bar{\mathcal{M}}^{\text{violation}}(\Lambda_b \to \Lambda_c^+\pi^-)\\
&= \frac{G_F}{\sqrt{2}}V_{cb}V_{ud}^*\Big(\mathcal{M}_a + \frac{1}{2}\mathcal{M}_b\Big).
\end{aligned} \tag{9}$$

In general, $\mathcal{M}_a$ and $\mathcal{M}_b$ are complex numbers, but the physical observables are the modulo square of the above equation, so it is trivial to notice that there are actually only three degrees of freedom, i.e., the physical observables depend only on the relative phase between $\mathcal{M}_a$ and $\mathcal{M}_b$. Therefore, the decay amplitude can be further parameterized as

$$\mathcal{M}_a = a, \quad \mathcal{M}_b = c + id, \tag{10}$$

with a, c, and d being the real fit parameters; the relative strength between the imaginary part d and the real part c describes the relative phase.

Analogously, one can obtain the decay amplitude of the $\Lambda_b^0 \to \Lambda_c^+ D^-$ process as shown in Fig. 2. Figure 2(a) maintains the light diquark structure and gives the amplitude

$$\bar{\mathcal{M}}^{\text{conserved}}(\Lambda_b^0 \to \Lambda_c^+ D^-) = \frac{G_F}{\sqrt{2}}V_{cb}V_{cd}^*\mathcal{M}_a. \tag{11}$$

Figure 2(b) breaks the light diquark structure and gives the amplitude

$$\bar{\mathcal{M}}^{\text{violation}}(\Lambda_b^0 \to \Lambda_c^+ D^-) = -\frac{1}{2}\frac{G_F}{\sqrt{2}}V_{cb}V_{cd}^*\mathcal{M}_b. \tag{12}$$

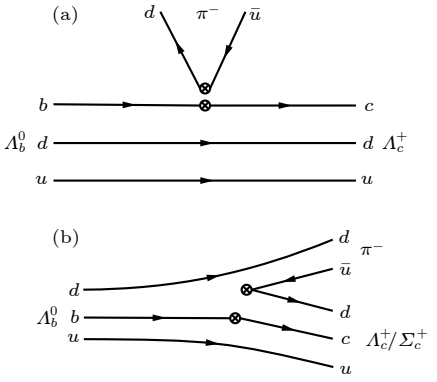

Fig. 1. The Feynman diagrams corresponding to the decays $\Lambda_b^0 \to \Lambda_c^+\pi^-$ and $\Lambda_b^0 \to \Sigma_c^+\pi^-$. [(a), (b)] The diquark conserved and violation diagrams, respectively. The diagrams for the Ξ_b^0 and Ξ_b^- decays are analogous. The crossed point is the effective weak decay vertex.

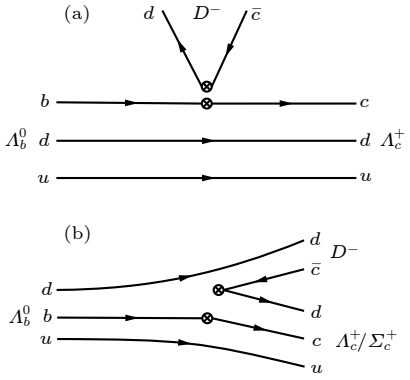

Fig. 2. The Feynman diagrams corresponding to the decays $\Lambda_b^0 \to \Lambda_c^+ D^-$ and $\Lambda_b^0 \to \Sigma_c^+ D^-$. [(a), (b)] The diquark conserved and violation diagrams, respectively. The diagrams for the Ξ_b^0 and Ξ_b^- decays are analogous. The crossed point is the effective weak decay vertex.

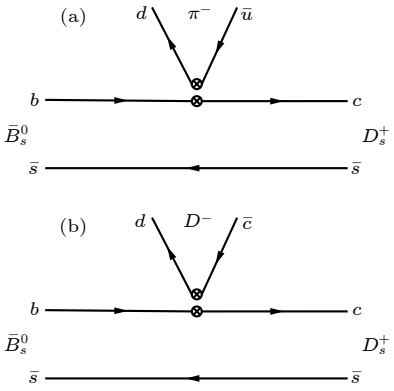

Fig. 3. The Feynman diagrams corresponding to the decays $\bar{B}_s^0 \to D_s^+\pi^-$ (a) and $\bar{B}_s^0 \to D_s^+ D^-$ (b). The diagrams for the $\bar{B}^0$ and B^- decays are analogous. The crossed point is the effective weak decay vertex.

The prefactor "$-\frac{1}{2}$" is from the recoupling

$$\begin{aligned}|ud_1\rangle_{(0,0)}|d_2\rangle_{(\frac{1}{2},-\frac{1}{2})} =& -\frac{1}{2}|ud_2\rangle_{(0,0)}|d_1\rangle_{(\frac{1}{2},-\frac{1}{2})} \\ &+\frac{\sqrt{3}}{2}|ud_2\rangle_{(1,1)}|d_1\rangle_{(\frac{1}{2},-\frac{1}{2})} \\ \Rightarrow& -\frac{1}{2}\Lambda_c^+ D^- + \frac{\sqrt{3}}{2}\Sigma_c^+ D^-. \end{aligned} \quad (13)$$

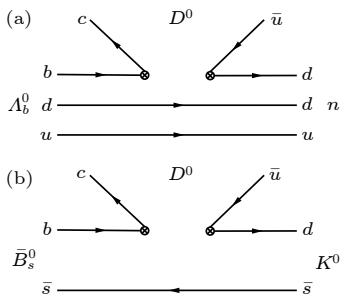

Fig. 4. The Feynman diagrams corresponding to the color-suppressed processes: (a) $\Lambda_b^0 \to nD^0$ and (b) $\bar{B}_s^0 \to K^0 D^0$.

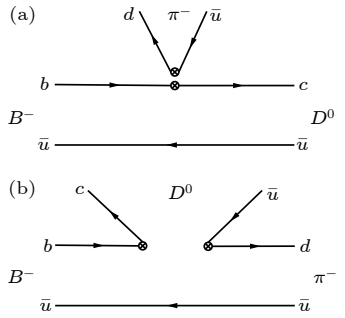

Fig. 5. The Feynman diagrams corresponding to the decay $B^- \to D^0\pi^-$. [(a), (b)] The color-favored and color-suppressed processes, respectively. By replacing the d quark with an s quark, one can obtain similar diagrams for $B^- \to D^0 K^-$.

The second d quark in $|d_2\rangle_{(\frac{1}{2},-\frac{1}{2})}$ is from the emitted W boson as shown in Fig. 2(b). Here, the $6-j$ symbol for the recoupling of three quarks is used, and the details can be found in Text A in the Supplementary Material. If the diquark picture works well, Figs. 1(a) and 2(a) correspond to the $\bar{B}_s^0 \to D_s^+\pi^-$ and $\bar{B}_s^0 \to D_s^+ D^-$ processes shown in Fig. 3. The decay $\bar{B}_s^0 \to K^0 D^0$ corresponds to the $\Lambda_b^0 \to nD^0$ in the light diquark picture shown in Fig. 4 and is a color-suppressed process, as the quark pair emitted from the W boson goes into different hadrons. As a result, another parameter F is considered to take into account the color-suppressed effect, and the amplitude reads

$$\bar{\mathcal{M}} = \frac{G_F}{\sqrt{2}} V_{cb}V_{ud}^* F \mathcal{M}_a. \quad (14)$$

Notably, there are both color-favored and color-suppressed processes for the decays $B^- \to D^0\pi^-$ and $B^- \to D^0 K^-$ presented in Fig. 5, so their amplitudes are written as

$$\bar{\mathcal{M}}(B^- \to D^0\pi^-) = \frac{G_F}{\sqrt{2}} V_{cb}V_{ud}^*(1+F)\mathcal{M}_a, \quad (15)$$

$$\bar{\mathcal{M}}(B^- \to D^0 K^-) = \frac{G_F}{\sqrt{2}} V_{cb}V_{us}^*(1+F)\mathcal{M}_a. \quad (16)$$

The decay amplitudes for other related processes can be found in Table 1. It is worth noting that the decay constant ratios $R_1 = f_K/f_\pi = 1.20$, $R_2 = f_D/f_\pi = 1.56$, and $R_3 = f_{D_s}/f_\pi = 1.98$[64] are multiplied to the corresponding channels to consider the effect of different final states on the diquark-conserved part amplitude $\mathcal{M}_a$, unless the decay channel is color-suppressed. This factor also takes into account the $SU(3)$ flavor symmetry breaking effect discussed in Refs. [65–67]. With these decay amplitudes,

one can obtain the corresponding decay widths via Eq. (2). It should be noted that our framework differs from the pQCD calculation [61] of the bottomed meson decays with explicitly considering the distribution amplitudes of the initial and final mesons, as well as the contribution of the other topological diagrams. In this work, we aim to test the extent to which the light diquark picture works for heavy baryon decays. Thus, we only consider the leading-order tree diagram contribution, but without the distribution amplitudes of the initial and final hadrons.

Table 1. The decay amplitudes of bottomed baryons and bottomed mesons.

Decay mode	Expression of $\bar{\mathcal{M}}$
$\Lambda_b^0 \to \Lambda_c^+ \pi^-$	$\frac{G_F}{\sqrt{2}} V_{cb}V_{ud}^*(\mathcal{M}_a + \frac{1}{2}\mathcal{M}_b)$
$\Lambda_b^0 \to \Sigma_c^+ \pi^-$	$\frac{G_F}{\sqrt{2}} V_{cb}V_{ud}^* \frac{1}{\sqrt{2}}\mathcal{M}_b$
$\Lambda_b^0 \to n D^0$	$\frac{G_F}{\sqrt{2}} V_{cb}V_{ud}^* F\mathcal{M}_a$
$\Lambda_b^0 \to \Lambda_c^+ D^-$	$\frac{G_F}{\sqrt{2}} V_{cb}V_{cd}^*(R_2\mathcal{M}_a - \frac{1}{2}\mathcal{M}_b)$
$\Lambda_b^0 \to \Sigma_c^+ D^-$	$\frac{G_F}{\sqrt{2}} V_{cb}V_{cd}^* \frac{\sqrt{3}}{2}\mathcal{M}_b$
$\bar{B}_s^0 \to D_s^+ \pi^-$	$\frac{G_F}{\sqrt{2}} V_{cb}V_{ud}^* \mathcal{M}_a$
$\bar{B}_s^0 \to D^0 K^0$	$\frac{G_F}{\sqrt{2}} V_{cb}V_{ud}^* F\mathcal{M}_a$
$\bar{B}_s^0 \to D_s^+ D^-$	$\frac{G_F}{\sqrt{2}} V_{cb}V_{cd}^* R_2\mathcal{M}_a$
$\Lambda_b^0 \to \Lambda_c^+ K^-$	$\frac{G_F}{\sqrt{2}} V_{cb}V_{us}^* R_1\mathcal{M}_a$
$\Lambda_b^0 \to \Lambda_c^+ D_s^-$	$\frac{G_F}{\sqrt{2}} V_{cb}V_{cs}^* R_3\mathcal{M}_a$
$\bar{B}_s^0 \to D_s^+ K^-$	$\frac{G_F}{\sqrt{2}} V_{cb}V_{us}^* R_1\mathcal{M}_a$
$\bar{B}_s^0 \to D_s^+ D_s^-$	$\frac{G_F}{\sqrt{2}} V_{cb}V_{cs}^* R_3\mathcal{M}_a$
$\Xi_b^0 \to \Xi_c^+ \pi^-$	$\frac{G_F}{\sqrt{2}} V_{cb}V_{ud}^* \mathcal{M}_a$
$\Xi_b^0 \to \Xi_c^+ K^-$	$\frac{G_F}{\sqrt{2}} V_{cb}V_{us}^* R_1\mathcal{M}_a$
$\Xi_b^0 \to \Xi_c^+ D^-$	$\frac{G_F}{\sqrt{2}} V_{cb}V_{cd}^* R_2\mathcal{M}_a$
$\Xi_b^0 \to \Xi_c^+ D_s^-$	$\frac{G_F}{\sqrt{2}} V_{cb}V_{cs}^* R_3\mathcal{M}_a$
$\bar{B}^0 \to D^+ \pi^-$	$\frac{G_F}{\sqrt{2}} V_{cb}V_{ud}^* \mathcal{M}_a$
$\bar{B}^0 \to D^+ K^-$	$\frac{G_F}{\sqrt{2}} V_{cb}V_{us}^* R_1\mathcal{M}_a$
$\bar{B}^0 \to D^+ D^-$	$\frac{G_F}{\sqrt{2}} V_{cb}V_{cd}^* R_2\mathcal{M}_a$
$\bar{B}^0 \to D^+ D_s^-$	$\frac{G_F}{\sqrt{2}} V_{cb}V_{cs}^* R_3\mathcal{M}_a$
$\Xi_b^- \to \Xi_c^0 \pi^-$	$\frac{G_F}{\sqrt{2}} V_{cb}V_{ud}^*(\mathcal{M}_a + \mathcal{M}_b)$
$\Xi_b^- \to \Xi_c^0 K^-$	$\frac{G_F}{\sqrt{2}} V_{cb}V_{us}^* R_1\mathcal{M}_a$
$\Xi_b^- \to \Xi_c^0 D^-$	$\frac{G_F}{\sqrt{2}} V_{cb}V_{cd}^*(R_2\mathcal{M}_a + \mathcal{M}_b)$
$\Xi_b^- \to \Xi_c^0 D_s^-$	$\frac{G_F}{\sqrt{2}} V_{cb}V_{cs}^* R_3\mathcal{M}_a$
$B^- \to D^0 \pi^-$	$\frac{G_F}{\sqrt{2}} V_{cb}V_{ud}^*(1+F)\mathcal{M}_a$
$B^- \to D^0 K^-$	$\frac{G_F}{\sqrt{2}} V_{cb}V_{us}^*(R_1+F)\mathcal{M}_a$
$B^- \to D^0 D^-$	$\frac{G_F}{\sqrt{2}} V_{cb}V_{cd}^* R_2\mathcal{M}_a$
$B^- \to D^0 D_s^-$	$\frac{G_F}{\sqrt{2}} V_{cb}V_{cs}^* R_3\mathcal{M}_a$

Results and Discussions. After fitting into the experimental decay widths of $\Lambda_b^0 \to \Lambda_c^+\pi^-/\Lambda_c^+D^-/\Lambda_c^+D_s^-$ and $\bar{B}_s^0 \to D_s^+\pi^-/D_s^+D^-/D^0K^0$, we obtain our fit results (as shown in Fig. 6) and the values of the parameters (as shown in Table 2). As shown in Fig. 6, our model describes the experimental data with $\chi^2/n_{\rm dof} = 1.2$. The fitted data match well with the experimental data, and the reason why $\chi^2/n_{\rm dof}$ is not very small is that the accuracy of the experimental measurements varies considerably from one channel to another, and our model ignores some higher-order corrections for the different channels. The value of the dimensionless parameter F is 0.372 ± 0.039, the absolute value of which is approximate to the factor 1/3, reflecting the color-suppressed contribution. Since $|\mathcal{M}_a| : |\mathcal{M}_b| = 1.973 : \sqrt{(-0.63)^2 + 4.09^2} \approx 0.476$, the diquark model is greatly violated in these heavy hadron decays, which supports the theory that the light diquark violated channel, i.e., $\Sigma_c^{(*)}\bar{D}^{(*)}$ channels, could be produced in Λ_b^0 decays with a sizable amplitude. The corresponding branching ratio between the $\Sigma_c^+D^-$ and the $\Lambda_c^+D^-$ channels,

$$\frac{\mathcal{B}r(\Lambda_b^0 \to \Sigma_c D^-)}{\mathcal{B}r(\Lambda_b^0 \to \Lambda_c D^-)} = 0.78, \tag{17}$$

also indicates that the peak structures in $\Lambda_b \to \Sigma_c^*\bar{D}^{(*)}K^- \to J/\Psi pK^-$ could be viewed as the $\Sigma_c^{(*)}\bar{D}^{(*)}$ hadronic molecular candidates. Several realistic fits [24,30,31,68] to the $J/\psi p$ invariant mass distribution and a recent lattice calculation [27] also demonstrate that the $\Sigma_c^{(*)}\bar{D}^{(*)}$ channels are the dominant channels for the formation of hidden charm pentaquarks.

Table 2. The value of each parameter in our fit.

Parameter	Value
a [GeV^3]	1.973 ± 0.04
c [GeV^3]	-0.63 ± 0.42
d [GeV^3]	4.09 ± 0.39
F(dimensionless)	0.372 ± 0.039

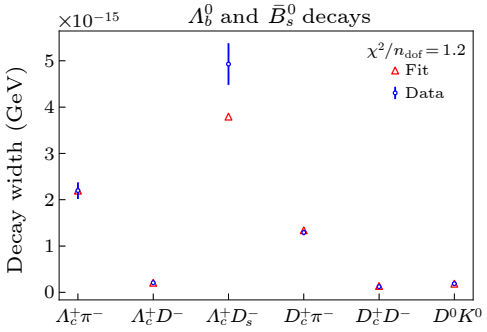

Fig. 6. The fitted decay widths with $\chi^2/n_{\rm dof} = 1.2$ compared with the experimental data. The blue circles are the experimental values. The red triangles are our results.

With the fitted parameters, one can predict the decay widths of the diquark-violated decays, i.e., $\Lambda_b^0 \to \Sigma_c^+\pi^-$ and $\Lambda_b^0 \to \Sigma_c^+D^-$, as shown in Table 3. As the charged pion can be detected directly in the detector, it is easier to measure the former one. The predicted width of the $\bar{B}_s^0 \to D_s^+K^-$ process is in good agreement with the experimental data within the margin of error, whereas the predicted width of $\bar{B}_s^0 \to D_s^+D_s^-$ is much larger than the experimental data and that of $\Lambda_b^0 \to \Lambda_c^+K^-$ is smaller than the experimental one, which is mainly due to neglect of the other topological diagrams and the rough treatment of the decay constant ratios between different decay channels in our model. Further experimental inputs, especially the three hadron decays, will give us a profound understanding of the diquark model and the dynamics of the exotic hadrons. Under $SU(3)$ symmetry, the Cabibbo-allowed decay widths of the Ξ_b^0, Ξ_b^-, $\bar{B}^0$, and B^- are also calculated, and are shown in Table 3. Apart from that, our calculations of the $\bar{B}^0 \to D^+\pi^-$ and $B^- \to D^0D^-$ decays are in good agreement with the current experimental

data within the errors, which can be seen easily from Table 3. Some other decays that cannot be well described by our model are probably due to the significant effect of higher-order contributions such as annihilation, penguin, and W-exchanged diagrams, the rough treatment of decay constant ratios between different decays, and the effect of the distribution amplitudes of the initial and final hadrons. The errors in Table 3 are estimated according to Eq. (2), i.e., the total error of the decay width is from the uncertainties of the input masses and parameters. The error of momentum for the predicted decays can be calculated via

$$\Delta|\boldsymbol{p}| = \Big[\Big(\frac{\partial|\boldsymbol{p}|}{\partial M}\cdot\Delta M\Big)^2 + \Big(\frac{\partial|\boldsymbol{p}|}{\partial m_1}\cdot\Delta m_1\Big)^2 + \Big(\frac{\partial|\boldsymbol{p}|}{\partial m_2}\cdot\Delta m_2\Big)^2\Big]^{\frac{1}{2}},$$

with M, m_1, and m_2 being the masses of the initial and final hadrons. Since the errors from masses, momentum, and G_F are very tiny, we ignore their contributions to the total errors of the final results. Thus, the error of each decay width Γ_i reads

$$\Delta\Gamma_i = \Big[\Big(\frac{\partial\Gamma_i}{\partial V_{cb}}\cdot\Delta V_{cb}\Big)^2 + \Big(\frac{\partial\Gamma_i}{\partial V_{qq'}}\cdot\Delta V_{qq'}\Big)^2 + \Big(\frac{\partial\Gamma_i}{\partial a}\cdot\Delta a\Big)^2 + \Big(\frac{\partial\Gamma_i}{\partial c}\cdot\Delta c\Big)^2 + \Big(\frac{\partial\Gamma_i}{\partial d}\cdot\Delta d\Big)^2 + \Big(\frac{\partial\Gamma_i}{\partial F}\cdot\Delta F\Big)^2\Big]^{\frac{1}{2}}. \quad (18)$$

The details of each error can be found in Text D in the Supplementary Material.

Table 3. The predicted widths, errors, and corresponding experimental data of each decay mode (units: GeV). These inputs correspond to the processes fitted in Fig. 6.

Decay mode	Γ_i (theory)	Error	Γ_i (experiment)
$\Lambda_b^0 \to \Lambda_c^+\pi^-$	–	–	$(2.20\pm0.18)\times10^{-15}$ (input)
$\Lambda_b^0 \to \Lambda_c^+ D^-$	–	–	$(2.06\pm0.27)\times10^{-16}$ (input)
$\bar{B}_s^0 \to D_s^+\pi^-$	–	–	$(1.30\pm0.06)\times10^{-15}$ (input)
$\bar{B}_s^0 \to D^0 K^0$	–	–	$(1.86\pm0.39)\times10^{-16}$ (input)
$\bar{B}_s^0 \to D_s^+ D^-$	–	–	$(1.21\pm0.22)\times10^{-16}$ (input)
$\Lambda_b^0 \to \Sigma_c^+\pi^-$	2.63×10^{-15}	5.29×10^{-16}	–
$\Lambda_b^0 \to n D^0$	1.75×10^{-16}	3.93×10^{-17}	–
$\Lambda_b^0 \to \Sigma_c^+ D^-$	1.60×10^{-16}	3.26×10^{-17}	–
$\Lambda_b^0 \to \Lambda_c^+ K^-$	9.31×10^{-17}	7.45×10^{-18}	$(1.60\pm0.13)\times10^{-16}$
$\Lambda_b^0 \to \Lambda_c^+ D_s^-$	–	–	$(4.93\pm0.45)\times10^{-15}$ (input)
$\bar{B}_s^0 \to D_s^+ K^-$	1.01×10^{-16}	8.09×10^{-18}	$(9.76\pm0.52)\times10^{-17}$
$\bar{B}_s^0 \to D_s^+ D_s^-$	4.14×10^{-15}	3.34×10^{-16}	$(1.91\pm0.22)\times10^{-15}$
$\Xi_b^0 \to \Xi_c^+\pi^-$	1.17×10^{-15}	9.36×10^{-17}	–
$\Xi_b^0 \to \Xi_c^+ K^-$	8.86×10^{-17}	7.09×10^{-18}	–
$\Xi_b^0 \to \Xi_c^+ D^-$	1.19×10^{-16}	1.04×10^{-17}	–
$\Xi_b^0 \to \Xi_c^+ D_s^-$	3.61×10^{-15}	2.92×10^{-16}	–
$\bar{B}^0 \to D^+\pi^-$	1.38×10^{-15}	1.10×10^{-16}	$(1.35\pm0.035)\times10^{-15}$
$\bar{B}^0 \to D^+ K^-$	1.04×10^{-16}	8.31×10^{-18}	$(8.90\pm0.35)\times10^{-17}$
$\bar{B}^0 \to D^+ D^-$	1.39×10^{-16}	1.22×10^{-17}	$(9.16\pm0.78)\times10^{-17}$
$\bar{B}^0 \to D^+ D_s^-$	4.25×10^{-15}	3.43×10^{-16}	$(3.12\pm0.35)\times10^{-15}$
$\Xi_b^- \to \Xi_c^0\pi^-$	7.08×10^{-15}	1.26×10^{-15}	–
$\Xi_b^- \to \Xi_c^0 K^-$	8.85×10^{-17}	7.09×10^{-18}	–
$\Xi_b^- \to \Xi_c^0 D^-$	3.81×10^{-16}	6.34×10^{-17}	–
$\Xi_b^- \to \Xi_c^0 D_s^-$	3.61×10^{-15}	2.91×10^{-16}	–
$B^- \to D^0\pi^-$	2.59×10^{-15}	2.54×10^{-16}	$(1.88\pm0.05)\times10^{-15}$
$B^- \to D^0 K^-$	1.78×10^{-16}	1.68×10^{-17}	$(1.48\pm0.06)\times10^{-16}$
$B^- \to D^0 D^-$	1.40×10^{-16}	1.22×10^{-17}	$(1.53\pm0.16)\times10^{-16}$
$B^- \to D^0 D_s^-$	4.26×10^{-15}	3.43×10^{-16}	$(3.62\pm0.36)\times10^{-15}$

In summary, numerous exotic candidates have been observed in experiments since the observation of $X(3872)$ in 2003. Their invariant mass distributions depend not only on the underlying formation dynamics but also on the production mechanism.[53] Many of them are observed in bottomed hadron decays, such as the hidden charm pentaquarks observed in Λ_b decays or the $X(3872)$ observed in B decays. As a result, the study of bottomed hadron decays provides a key ingredient in the study of the properties of exotic hadrons. We examine the two-hadron decays of bottomed baryons and bottomed mesons to probe to what extent the light diquark picture works. This places a constraint on the properties of the exotic candidates observed in bottomed hadron decays. Our results show that the diquark picture is greatly violated in these decays, since the diquark violated amplitude is significantly larger than the diquark conserved one. Furthermore, several theoretical studies of the hidden pentaquarks disagree on whether the hidden charm pentaquark dominant channels $\Sigma_c^{(*)}\bar{D}^{(*)}$ could be produced in Λ_b^0 decays with sizable production rates or not. This is crucial for its line shape, i.e., whether it has peak structures or dip structures.[53] Our work indicates that Λ_b has a significant probability of decay into Σ_c, which offers evidence that the hidden charm pentaquarks could express themselves as peaks in Λ_b decays. In addition, the decay widths of the $\Lambda_b^0 \to \Sigma_c^+\pi^-$ and $\Lambda_b^0 \to \Sigma_c^+ D^-$ processes are also predicted, which can be measured in the forthcoming ex-

periments. We also find that the predicted width of the $\bar{B}_s^0 \to D_s^+ K^-$ process is in good agreement with the experimental data within the margin of error, whereas the predicted width of $\bar{B}_s^0 \to D_s^+ D_s^-$ is much larger than the experimental data and that of $\Lambda_b^0 \to \Lambda_c^+ K^-$ is smaller than the experimental one, probably due to the neglect of the other topological diagrams and the rough treatment of the decay constant ratios between different decays in our model.

Acknowledgements. We are grateful to Qiang Zhao for helpful discussion. This work was partly supported by the National Natural Science Foundation of China (Grant Nos. 12375073, 12035007, 12205106, and 12105028), Guangdong Provincial Fund (Grant No. 2019QN01X172), Guangdong Major Project of Basic and Applied Basic Research (Grant No. 2020B0301030008), the NSFC and the Deutsche Forschungsgemeinschaft (DFG, German Research Foundation) through the funds provided to the Sino-German Collaborative Research Center TRR110 "Symmetries and the Emergence of Structure in QCD" (NSFC Grant No. 12070131001, DFG Project-ID 196253076-TRR 110). D.C.Y. was also supported by the Natural Science Foundation of Jiangsu Province (Grant No. BK20200980).

References

[1] Gell M M 2019 *Resonance* **24** 923
[2] Zweig G 1964 CERN-TH-401
[3] Choi S K *et al.* [Belle] 2003 *Phys. Rev. Lett.* **91** 262001
[4] Uehara S *et al.* [Belle] 2006 *Phys. Rev. Lett.* **96** 082003
[5] Aaltonen T *et al.* [CDF] 2009 *Phys. Rev. Lett.* **102** 242002
[6] Aaij R *et al.* [LHCb] 2017 *Phys. Rev. Lett.* **118** 022003
[7] Aaij R *et al.* [LHCb] 2019 *Phys. Rev. Lett.* **122** 222001
[8] Olsen S L, Skwarnicki T, and Zieminska D 2018 *Rev. Mod. Phys.* **90** 015003
[9] Yuan C Z 2019 *EPJ Web Conf.* **202** 01004
[10] Yuan C Z, and Olsen S L 2019 *Nat. Rev. Phys.* **1** 480
[11] Brambilla N *et al.* 2020 *Phys. Rep.* **873** 1
[12] Robertson G [LHCb] 2022 arXiv:2107.14560 [hep-ex]
[13] Fang B [LHCb] 2022 *Nucl. Part. Phys. Proc.* **318–323** 66
[14] Chen S Z *et al.* 2023 *Front. Phys.* **18** 44601
[15] Zhang J Q [CMS] 2023 *Proc. Sci.* **445** 088
[16] Liu Z Q and Mitchell R E 2023 *Sci. Bull.* **68** 2148
[17] Jia S, Xiong W T, and Shen C P 2023 *Chin. Phys. Lett.* **40** 121301
[18] Wu J J, Molina R, Oset E, and Zou B S 2010 *Phys. Rev. Lett.* **105** 232001
[19] Wang W L, Huang F, Zhang Z Y, and Zou B S 2011 *Phys. Rev. C* **84** 015203
[20] Wu J J, Lee T S H, and Zou B S 2012 *Phys. Rev. C* **85** 044002
[21] Xiao C W, Nieves J, and Oset E 2013 *Phys. Rev. D* **88** 056012
[22] Karliner M and Rosner J L 2015 *Phys. Rev. Lett.* **115** 122001
[23] Liu M Z *et al.* 2019 *Phys. Rev. Lett.* **122** 242001
[24] Du M L, Baru V, Guo F K, Hanhart C, Meißner U G, Oller J A, and Wang Q 2020 *Phys. Rev. Lett.* **124** 072001
[25] Peng F Z, Yan M J, Sánchez M S, and Valderrama M P 2023 *Phys. Lett. B* **846** 138207
[26] Yang Z Y, Peng F Z, Yan M J, Sánchez M S, and Valderrama M P 2022 arXiv:2211.08211 [hep-ph]
[27] Xing H Y, Liang J, Liu L M, Sun P, and Yang Y B 2022 arXiv:2210.08555 [hep-lat]
[28] Yalikun N, Lin Y H, Guo F K, Kamiya Y, and Zou B S 2021 *Phys. Rev. D* **104** 094039
[29] Yan M J, Peng F Z, Sánchez M S, and Valderrama M P 2022 *Eur. Phys. J. C* **82** 574
[30] Du M L, Baru V, Guo F K, Hanhart C, Meißner U G, Oller J A, and Wang Q 2021 *J. High Energ. Phys.* **2021** 157
[31] Kuang S Q, Dai L Y, Kang X W, and Yao D L 2020 *Eur. Phys. J. C* **80** 433
[32] Pan Y W, Liu M Z, Peng F Z, Sánchez M S, Geng L S, and Valderrama M P 2020 *Phys. Rev. D* **102** 011504
[33] Liu M Z, Wu T W, Sánchez M S, Valderrama M P, Geng L S, and Xie J J 2021 *Phys. Rev. D* **103** 054004
[34] Wang F L, Chen R, Liu Z W, and Liu X 2020 *Phys. Rev. C* **101** 025201
[35] Chen R, Sun Z F, Liu X, and Zhu S L 2019 *Phys. Rev. D* **100** 011502
[36] Wang B, Meng L, and Zhu S L 2019 *J. High Energ. Phys.* **2019** 108
[37] Chen H X, Chen W, and Zhu S L 2019 *Phys. Rev. D* **100** 051501
[38] Guo F K, Jing H J, Meißner U G, and Sakai S 2019 *Phys. Rev. D* **99** 091501
[39] He J 2019 *Eur. Phys. J. C* **79** 393
[40] Guo Z H and Oller J A 2019 *Phys. Lett. B* **793** 144
[41] Shimizu Y, Yamaguchi Y, and Harada M 2019 arXiv:1904.00587 [hep-ph]
[42] Xiao C J, Huang Y, Dong Y B, Geng L S, and Chen D Y 2019 *Phys. Rev. D* **100** 014022
[43] Xiao C W, Nieves J, and Oset E 2019 *Phys. Rev. D* **100** 014021
[44] Meng L, Wang B, Wang G J, and Zhu S L 2019 *Phys. Rev. D* **100** 014031
[45] Wu J J, Lee T S H, and Zou B S 2019 *Phys. Rev. C* **100** 035206
[46] Xiao C W, Nieves J, and Oset E 2019 *Phys. Lett. B* **799** 135051
[47] Voloshin M B 2019 *Phys. Rev. D* **100** 034020
[48] Sakai S, Jing H J, and Guo F K 2019 *Phys. Rev. D* **100** 074007
[49] Yamaguchi Y, Garcia T H, Giachino A, Hosaka A, Santopinto E, Takeuchi S, and Takizawa M 2020 *Phys. Rev. D* **101** 091502
[50] Lin Y H and Zou B S 2019 *Phys. Rev. D* **100** 056005
[51] Gutsche T and Lyubovitskij V E 2019 *Phys. Rev. D* **100** 094031
[52] Burns T J and Swanson E S 2019 *Phys. Rev. D* **100** 114033
[53] Dong X K, Guo F K, and Zou B S 2021 *Phys. Rev. Lett.* **126** 152001
[54] Liu X H, Wang Q, and Zhao Q 2016 *Phys. Lett. B* **757** 231
[55] Burns T J and Swanson E S 2022 *Phys. Rev. D* **106** 054029
[56] Workman R L *et al.* [PDG] 2022 *Prog. Theor. Exp. Phys.* **2022** 083C01
[57] Leibovich A K, Ligeti Z, Stewart I W, and Wise M B 2004 *Phys. Lett. B* **586** 337
[58] Fan Y Y, Wang W F, Cheng S, and Xiao Z J 2013 *Phys. Rev. D* **87** 094003
[59] Zhang C Q, Li J M, Jia M K, and Rui Z 2022 *Phys. Rev. D* **105** 073005
[60] Buchalla G, Buras A J, and Lautenbacher M E 1996 *Rev. Mod. Phys.* **68** 1125
[61] Li R H, Lü C D, and Zou H 2008 *Phys. Rev. D* **78** 014018
[62] Wang W, Yu F S, and Zhao Z X 2017 *Eur. Phys. J. C* **77** 781
[63] Ke H W, Lu F, Liu X H, and Li X Q 2020 *Eur. Phys. J. C* **80** 140
[64] Chang Q, Li X N, Li X Q, and Su F 2018 *Chin. Phys. C* **42** 073102
[65] Qin Q, Li H, Lü C D, and Yu F S 2014 *Phys. Rev. D* **89** 054006
[66] Jia C P, Wang D, and Yu F S 2020 *Nucl. Phys. B* **956** 115048
[67] Huber T and Tetlalmatzi X G 2022 *Eur. Phys. J. C* **82** 210
[68] Nakamura S X, Hosaka A, and Yamaguchi Y 2021 *Phys. Rev. D* **104** L091503